**Research Article** **ISSN: 2395 – 5597**

# International Journal of Engineering and Robot Technology

**Journal home page: www.ijerobot.com**

## COMPARISON OF 2-D AND 3-D EFFECTS ON VARIOUS GEOMETRY TO PREDICT THE EFFECTIVE THERMAL CONDUCTIVITY OF POROUS SYSTEM

**Senthil Kumar A. P*[1], S. Janaki[2], N. Jagadeesh[3], R. Selladurai[4], T. Sakthivel[4]**

[1]*Department of Mechanical Engineering, PSG, College of Technology, Coimbatore, India.
[2]Department of Mechanical Engineering, Akshaya College of Engineering and Technology, Coimbatore, India.
[3]Department of Mechanical Engineering, PSG CT, Coimbatore, India.
[4]Department of Mechanical, PSG Polytechnic College, Coimbatore, India.

**ABSTRACT**
In this article, the 3-Dimensional numerical model has been developed for estimating effective thermal conductivity of porous system based on unit cell approach. The inherent 3-D problem is modeled using Finite Element Analysis for various inclusions (square, circular, hexagon and octagon). The model is tested with at different composition of solid to fluid fractions and solid to fluid conductivities. Comparison has been carried out for 2-Dimensioanl and 3-Dimensional effect for various inclusions for estimating the effective thermal conductivity of porous materials. The results shows that for higher concentration and conductivity ratio, the model with varying cross section estimates the effective thermal conductivity of two phase materials with higher accuracy.

**KEYWORDS**
Index Terms-2D-3D dimensional, Various inclusions, Conductivity ratio, Contact ratio, Porous systems and Concentration.

**Author for Correspondence:**

Senthil Kumar A P,

Department of Mechanical Engineering,

PSG, College of Technology, Coimbatore, India.

**Email:** apspsgct@yahoo.com

## INTRODUCTION

The theoretical estimation of the effective thermal conductivity (ETC) of two phase materials has been always difficult. Use of two-phase materials is regarded as more effective means of energy conservation and energy efficiency in an industrial sector. Numerous models were developed to find out the effective conductivity of mixtures, but one of the major limitations of the models is its suitability for specific application. Effective thermal conductivity of two phase material is very important to determine

heat transfer characteristics. Reddy and Karthikeyan[1] developed the collocated parameter model based on the unit cell approach for predicting the effective thermal conductivity of the two-phase materials. Tai[2] deduced mathematical expressions for the equivalent thermal conductivity of two and three-dimensional orthogonally fiber-reinforced composites in a one-dimensional heat flow model. In this regard, Tai applied the fundamental definitions of thermal conductivity and the simple rule of mixtures to a unit cell of an orthogonally fiber-reinforced material. Tai, showed that whether a square slab model or a cylindrical fiber model is used makes little difference to the heat flux; while the fiber volume fraction matters. Jones and Pascal[3] developed a three-dimensional numerical finite-difference to calculate the thermal conductivity of a composite with two or more constituents to better understand how the relative quantities and distributions of the component materials, within a sample, affect the whole sample conductivity. Graham and McDowell[4] estimated the transverse thermal conductivity of continuous reinforced composites containing a random fiber distribution with imperfect interfaces using finite-element analysis. Krach and Advani[5] investigated the effect of void volume and shape on the effective conductivity of a unidirectional sample of a 3-phase composite using a numerical approach consisting of a unit cell. Their findings clearly showed that the influence of porosity on thermal conductivity could not be described solely by the void volume. They found that the shape and distribution of the voids influence the effective thermal conductivity. Al-Sulaiman *et al*[6] developed correlations based on a finite element analysis that predict the thermal conductivity of fibers utilizing the easy to measure thermal conductivity of the Fiber Reinforced Composite Laminates (FRCL) and the other constituents. In their model, Al-Sulaiman *et al* considered the FRCL cured at high pressures such that it includes no air voids. Zou *et al*[7]. Come up with an analytical expression for transverse thermal conductivities of unidirectional fiber composites with and without thermal barrier is derived based on the electrical analogy technique and on the cylindrical filament-square packing array unit cell model (C-S model). The effective thermal conductivity modeling of various inclusions has been carried out by A P Senthil Kumar[8-9].

**Symbols**

$\alpha$ Conductivity ratio($k_s/k_f$),
$\upsilon$ Concentration
$\lambda$ Contact ratio(c/a)
A Wall area ($m^2$)
h Heat transfer coefficient ($W/m^2.K$)
$T_{conv}$ bulk temperature of the fluid at the convection side (K)
$T_{wall1}$ fixed wall temperature (K)
$T_{wall2}$ convective wall temperature (K).

## NUMERICAL ANALYSIS FOR VARIOUS INCLUSIONS

Numerical heat transfer analysis of the unit cell for various inclusion shapes (square, hexagon, octagon and circular cylinders) has been carried out to estimate the ETC of porous materials via the Finite Element simulation. For this heat transfer analysis ANSYS, a finite element software package is used. Solid 90 element was used for the analysis and an element size of 0.03 was adopted. Software validation and mesh sensitivity test has been carried out

**Boundary condition**

One face of the unit cell is subjected to constant temperature and the opposite face is subjected to convective thermal environment. All other faces are kept as adiabatic in order to achieve 1D heat transfer. The boundary condition imposed on the unit cell is shown in the Figure No.1.

**Determination of Effective Thermal conductivity**

From the results of the finite element analysis, the average surface temperature on the convection wall of the unit cell is computed. Once the temperature of the convective side is known, the effective thermal conductivity across the two walls can be calculated using the following simple heat balance equation

$$hA\left(T_{wall\,2}-T_{conv}\right)=\frac{K_{eff}A\left(T_{wall1}-T_{wall\,2}\right)}{L} \qquad (1)$$

**Mesh sensitivity test**

Figure No.2. Shows the meshed model of the unit cell of the square cylinder. Three iterations have been carried out for the case of two-phase material

with conductivity ratio (α) = 800, concentration (υ) = 0.5 and contact ratio (λ) = 0.02 for mesh-independent study. The finite element edge size was changed from very coarse to very fine, when performing the iterations. In each of these three runs, the average temperature at the convective wall of the two-phase material was obtained.

A summary of the results of iterations indicating the element edge size and the corresponding average wall temperature obtained for various inclusions is shown in Table No.1. It is observed that the average wall temperature remains almost constant after using an element edge size of 0.1, indicating the convergence of the solution. Hence, an element edge size of 0.1 is used for further analysis.

## THREE - DIMENSIONAL MODELING FOR VARIOUS INCLUSIONS BASED ON PRIMARY AND SECONDARY PARAMETERS

A model with 3-Dimensional effect has been considered to estimate the ETC of porous materials. The unit cell of various inclusion shapes (square, circular, octagon and hexagon cylinder) has been modeled parametrically. The numerical modeling has been carried out for various inclusions by considering the primary and secondary parameters, viz., conductivity ratio, concentration and contact ratio. The inclusion shapes namely, square, hexagon, octagon having a side length of 'a' having a contact cube of side length 'c'. Similarly, circular cylinders having diameter 'a' and an inline contact plate of width 'c' and height 'δ'. The finite contact between the cylinders by connecting plates is denoted the contact parameter 'c/a'. Because of the symmetry of the plates, one fourth of the cross-section has been considered as a unit cell for all shapes of inclusions and is shown in Figure No.3 (a-d). For all inclusions, the first layer consists of solid phase with a dimension of (c/2) $(l/2)^2$. The second layer consists of solid and fluid phases dimensions of ((a-c)/2) $(a/2)^2$ and ((a-c)/2) $((l\text{-}a)/2)^2$ for square cylinder. For third layer consists of solid and fluid phases dimensions of $((l\text{-}a)/2)$ $(c/2)^2$ and $((l\text{-}a)/2)$ $((l\text{-}c)/2)^2$ for square cylinder. Similarly, for circular cylinder the second and third layer consists of solid and fluid phases dimensions of ((a-c)/2) $(a/2)^2$ & ((a-c)/2) $((l\text{-}a)/2)^2$, and (δ/2) $(c/2)^2$ and (δ/2) $(l\text{-}c/2)^2$ respectively. For octagon cylinder the second and third layer consists of solid and fluid phases dimensions of {[a/2 + a/√2]-c/2} $(a/2 + a/\sqrt{2})^2$ and {[a/2 + a/√2]-c/2} $(l/2\text{-}(a/2+a/\sqrt{2}))^2$ and $(l/2\text{-}(a/2+a/\sqrt{2}))$ $(c/2)^2$ and $(l/2\text{-}(a/2+a/\sqrt{2}))$ $(l\text{-}c/2)^2$ respectively. Similarly, for hexagon cylinder the second and third layer consists of solid and fluid phases dimensions of [a√3/2-c/√2] $(a/2+\{a/\sqrt{2}\text{-}c/2\sqrt{3}\})^2$ & [a√3/2-c/√2] $(l/2\text{-}(a/2+\{a/\sqrt{2}\text{-}c/2\sqrt{3}\})^2$ and $(l/2\text{-}(a\sqrt{3}/2))$ $(c/2)^2$ and $(l/2\text{-}(a\sqrt{3}/2))$ $(l\text{-}c/2)^2$ respectively.

## COMPARISON RESULTS OF 2-DIMESIONAL AND 3-DIMESIOANL EFFECTS ON NUMERICAL MODELING FOR VARIOUS INCLUSIONS WITH EXPERIMENTAL DATA

The numerically predicted effective thermal conductivity values for square, hexagon, octagon and circular cylinders models have been compared with published experimental data for porous granular materials and found that 3-dimensional numerical values predicted are quite close to the experimental results with high accuracy. A comparison of 2-dimensional and 3- dimensional numerical models with experimental data for different concentrations and conductivity ratios has been made for porous materials and is given in the Table No.1 (a-b). Experimental data for various two-phase systems were taken from reported studies. For porous granular materials [υ = 0.2 to 0.740 and α = 7.368 to 233.653], the 3-Dimensional circular cylinder model having very close agreement with the experimental data compared with other geometry's. The range of accuracy appears quite good in consideration with the variety of sources of data selected and the wide range of shapes included. It is observed that the 3-Dimensional circular cylinder model has an average deviation of ± 1.89 % from experimental data as against ± 6.67 % of square cylinder, ± 4.97 % of hexagon cylinder and ± 3.07 % of octagon cylinder respectively with 3-Dimesional effect Table No.2 (a-b). For the same range, 2-Dimesional numerical model having the minimum and maximum deviation of ± 43.53 % and ± 57.95 % respectively for various inclusions is shown in Table No.1 (a-b). It is clearly indicate that the 3-Dimensional numerical model is

predicting the effective thermal conductivity better than the 2-Dimensional numerical model for consideration of same concentration, conductivity and contact ratios. This is due to the effect of solid conductivity on the fluid phase on the 2-dimensional numerical model.

**Table No.1: Mesh sensitivity test**

| S.No | Element edge size | Average temperature °C | | | |
|---|---|---|---|---|---|
| | | Square cylinder | Circular cylinder | Hexagon cylinder | Octagon cylinder |
| 1 | 0.5 | 347.8 | 348.8 | 347.9 | 348.0 |
| 2 | 0.2 | 345.2 | 345.8 | 345.2 | 345.6 |
| 3 | 0.1 | 344.8 | 344.9 | 344.8 | 344.6 |

**Table No.2: a. Comparison on two dimensional and three dimensional effects on numerical effective thermal conductivity with experimental data for porous system**

| S.No | Sample (solid/fluid phase) | $k_s$ | $k_f$ | α ($k_s/k_f$) | υ | $k_{exp}$ | λ (c/a) SQU | $k_{squ}$ | | | | Λ (c/a) CIR | $k_{cir}$ | | | |
|---|---|---|---|---|---|---|---|---|---|---|---|---|---|---|---|---|
| | | | | | | | | 3D | Devi | 2D | Devi | | 3D | Devi | 2D | Devi |
| 1 | Glass sphere/ air | 1.099 | 0.024 | 45.792 | 0.74 | 0.227 | 0.55 | 0.2283 | 0.584 | 0.614 | 63.03 | 0.63 | 0.225 | 1.01 | 0.654 | 65.29 |
| 2 | Glass sphere/ air | 1.099 | 0.024 | 45.792 | 0.2 | 0.041 | 0.03 | 0.0419 | 2.123 | 0.056 | 26.79 | 0.03 | 0.040 | 1.56 | 0.058 | 29.31 |
| 3 | Silica sphere/water | 12.414 | 0.586 | 21.184 | 0.569 | 2.544 | 0.43 | 2.3055 | 10.34 | 4.86 | 47.65 | 0.53 | 2.582 | 1.47 | 5.612 | 54.67 |
| 4 | Stainless steel/ eth.alcohol | 20.864 | 0.337 | 61.911 | 0.495 | 2.009 | 0.17 | 2.0303 | 1.049 | 4.459 | 54.95 | 0.21 | 2.017 | 0.39 | 6.078 | 66.95 |
| 5 | Glass sphere/ iso-octane | 1.061 | 0.144 | 7.368 | 0.57 | 0.406 | 0.01 | 0.3234 | 25.56 | 6.72 | 93.96 | 0.86 | 0.401 | 1.21 | 0.521 | 22.07 |
| 6 | Lead shots/helium | 34.347 | 0.147 | 233.65 | 0.62 | 2.14 | 0.1 | 2.1923 | 2.387 | 5.815 | 63.2 | 0.13 | 2.143 | 0.14 | 10.746 | 80.09 |
| 7 | Lead shots/hydrogen | 34.347 | 0.179 | 191.88 | 0.62 | 2.429 | 0.11 | 2.4042 | 1.033 | 7.161 | 66.08 | 0.15 | 2.390 | 1.63 | 11.507 | 78.89 |
| 8 | Lead shots/water | 34.347 | 0.627 | 54.78 | 0.62 | 5.404 | 0.38 | 5.4171 | 0.241 | 13.368 | 59.58 | 0.47 | 5.437 | 0.62 | 16.896 | 68.02 |
| 9 | Zircona powder/air | 2.001 | 0.021 | 95.286 | 0.47 | 0.12 | 0.08 | 0.1228 | 2.242 | 0.266 | 54.89 | 0.1 | 0.123 | 2.17 | 0.381 | 68.5 |
| 10 | Lead/water | 33.764 | 0.586 | 57.618 | 0.6 | 4.329 | 0.24 | 4.3473 | 0.422 | 4.617 | 6.238 | 0.33 | 4.344 | 0.36 | 14.95 | 71.04 |
| 11 | Zircona powder/air | 2.001 | 0.03 | 66.7 | 0.58 | 0.23 | 0.2 | 0.2315 | 0.655 | 0.561 | 59 | 0.27 | 0.228 | 0.69 | 0.397 | 42.07 |
| 12 | Zircona powder/air | 2.001 | 0.03 | 66.7 | 0.64 | 0.281 | 0.28 | 0.2817 | 0.253 | 0.728 | 61.4 | 0.4 | 0.283 | 0.86 | 1.02 | 72.45 |
| 13 | Zircona powder/air | 2.001 | 0.03 | 66.7 | 0.7 | 0.364 | 0.49 | 0.3676 | 0.977 | 0.99 | 63.23 | 0.58 | 0.363 | 0.17 | 1.188 | 69.36 |
| 14 | Glass beads/ air | 1.201 | 0.028 | 42.893 | 0.65 | 0.22 | 0.47 | 0.2206 | 0.263 | 0.543 | 59.48 | 0.55 | 0.224 | 1.93 | 0.643 | 65.79 |
| 15 | Glass beads/benzene | 1.201 | 0.14 | 8.579 | 0.65 | 0.5 | 0.49 | 0.3572 | 39.99 | 0.649 | 22.96 | 0.98 | 0.482 | 3.8 | 0.639 | 21.75 |
| 16 | Quartz sand/ water | 5.003 | 0.62 | 8.069 | 0.676 | 2.331 | 0.9 | 1.8049 | 29.15 | 2.816 | 17.22 | 0.98 | 2.082 | 12 | 2.789 | 16.42 |
| 17 | Glass beads/air | 1.091 | 0.029 | 37.621 | 0.6 | 0.18 | 0.35 | 0.1809 | 0.504 | 0.414 | 56.52 | 0.45 | 0.182 | 1.18 | 0.522 | 65.52 |
| 18 | Micro beads/air | 1.046 | 0.026 | 40.231 | 0.65 | 0.193 | 0.45 | 0.1930 | 0.022 | 0.47 | 58.94 | 0.55 | 0.198 | 2.37 | 0.562 | 65.66 |
| 19 | Micro beads/soltrol | 1.046 | 0.133 | 7.865 | 0.639 | 0.452 | 0.49 | 0.3198 | 41.34 | 0.565 | 20 | 0.98 | 0.426 | 5.99 | 0.556 | 18.71 |
| 20 | Wassau sand/ n-heptane | 8.374 | 0.129 | 64.915 | 0.485 | 0.722 | 0.13 | 0.7165 | 0.77 | 1.545 | 53.27 | 0.17 | 0.725 | 0.37 | 2.183 | 66.93 |
| 21 | Ottawa sand/ helium | 8.374 | 0.147 | 56.966 | 0.64 | 1.323 | 0.36 | 1.3225 | 0.036 | 3.342 | 60.41 | 0.46 | 1.310 | 0.97 | 4.336 | 69.49 |
| 22 | Wassau sand/ helium | 8.374 | 0.147 | 56.966 | 0.41 | 0.598 | 0.1 | 0.6031 | 0.851 | 1.156 | 48.27 | 0.12 | 0.598 | 0.01 | 1.535 | 61.04 |
| 23 | Miami silt loam/air | 2.932 | 0.023 | 127.48 | 0.456 | 0.169 | 0.08 | 0.1612 | 4.86 | 0.36 | 53.06 | 0.1 | 0.166 | 2.08 | 0.523 | 67.69 |
| 24 | Miami silt loam/air | 2.932 | 0.023 | 127.48 | 0.552 | 0.221 | 0.12 | 0.2227 | 0.75 | 0.571 | 61.3 | 0.16 | 0.226 | 2.14 | 0.861 | 74.33 |
| 25 | Glass/air | 1.13 | 0.026 | 43.462 | 0.6 | 0.176 | 0.32 | 0.1766 | 0.343 | 0.412 | 57.28 | 0.4 | 0.172 | 2.27 | 0.531 | 66.85 |
| Average deviation | | | | | | | | | 6.67 | | 51.55 | | | 1.89 | | 57.96 |

**Table No.2: b. Comparison on two dimensional and three dimensional effects on numerical effective thermal conductivity with experimental data for porous system**

| S.No | $k_s$ | $k_f$ | $\alpha$ ($k_s/k_f$) | $\upsilon$ | $k_{exp}$ | $\lambda$ (c/a) OCT | $k_{octa}$ | | | | $\lambda$ (c/a) HEX | $k_{hex}$ | | | |
|---|---|---|---|---|---|---|---|---|---|---|---|---|---|---|---|
| | | | | | | | 3D | Devi | 2D | Devi | | 3D | Devi | 2D | Devi |
| 1 | 1.099 | 0.024 | 45.792 | 0.74 | 0.227 | 0.7 | 0.227 | 0.007 | 0.541 | 58.04 | 0.85 | 0.2202 | 3.096 | 0.658 | 65.5 |
| 2 | 1.099 | 0.024 | 45.792 | 0.2 | 0.041 | 0.05 | 0.0403 | 1.851 | 0.051 | 19.61 | 0.05 | 0.0428 | 4.166 | 0.0584 | 29.79 |
| 3 | 12.414 | 0.586 | 21.184 | 0.569 | 2.544 | 0.81 | 2.5478 | 0.149 | 5.052 | 49.64 | 0.8 | 2.4224 | 5.018 | 5.2434 | 51.48 |
| 4 | 20.864 | 0.337 | 61.911 | 0.495 | 2.009 | 0.33 | 2.0036 | 0.267 | 4.718 | 57.42 | 0.27 | 2.049 | 1.955 | 4.927 | 59.22 |
| 5 | 1.061 | 0.144 | 7.368 | 0.57 | 0.406 | 0.33 | 0.3448 | 17.76 | 0.464 | 12.5 | 0.01 | 0.341 | 19.05 | 0.3812 | 6.506 |
| 6 | 34.347 | 0.147 | 233.65 | 0.62 | 2.14 | 0.22 | 2.1594 | 0.899 | 3.649 | 41.35 | 0.16 | 2.1634 | 1.084 | 5.755 | 62.81 |
| 7 | 34.347 | 0.179 | 191.88 | 0.62 | 2.429 | 0.25 | 2.428 | 0.042 | 3.897 | 37.67 | 0.18 | 2.409 | 0.832 | 5.231 | 53.57 |
| 8 | 34.347 | 0.627 | 54.78 | 0.62 | 5.404 | 0.69 | 5.3993 | 0.088 | 8.039 | 32.78 | 0.6 | 5.3867 | 0.322 | 14.618 | 63.03 |
| 9 | 2.001 | 0.021 | 95.286 | 0.47 | 0.12 | 0.17 | 0.1217 | 1.379 | 0.295 | 59.32 | 0.1 | 0.1105 | 8.592 | 0.257 | 53.31 |
| 10 | 33.764 | 0.586 | 57.618 | 0.6 | 4.329 | 0.45 | 4.3105 | 0.429 | 4.863 | 10.98 | 0.37 | 4.3178 | 0.26 | 6.398 | 32.34 |
| 11 | 2.001 | 0.03 | 66.7 | 0.58 | 0.23 | 0.41 | 0.2308 | 0.348 | 0.615 | 62.6 | 0.32 | 0.2311 | 0.478 | 0.628 | 63.38 |
| 12 | 2.001 | 0.03 | 66.7 | 0.64 | 0.281 | 0.55 | 0.2791 | 0.683 | 0.788 | 64.34 | 0.45 | 0.2793 | 0.622 | 0.816 | 65.56 |
| 13 | 2.001 | 0.03 | 66.7 | 0.7 | 0.364 | 0.9 | 0.3645 | 0.131 | 1.042 | 65.07 | 0.75 | 0.3533 | 3.037 | 1.07 | 65.98 |
| 14 | 1.201 | 0.028 | 42.893 | 0.65 | 0.22 | 0.79 | 0.2205 | 0.212 | 0.554 | 60.29 | 0.75 | 0.2209 | 0.412 | 0.586 | 62.46 |
| 15 | 1.201 | 0.14 | 8.579 | 0.65 | 0.5 | 0.05 | 0.4333 | 15.39 | 0.522 | 4.215 | 0.01 | 0.4275 | 16.96 | 0.471 | 6.157 |
| 16 | 5.003 | 0.62 | 8.069 | 0.676 | 2.331 | 0.05 | 2.0043 | 16.3 | 2.248 | 3.692 | 0.1 | 1.9254 | 21.06 | 2.399 | 2.835 |
| 17 | 1.091 | 0.029 | 37.621 | 0.6 | 0.18 | 0.63 | 0.1814 | 0.794 | 0.619 | 70.92 | 0.6 | 0.1848 | 2.612 | 0.46 | 60.87 |
| 18 | 1.046 | 0.026 | 40.231 | 0.65 | 0.193 | 0.75 | 0.1923 | 0.346 | 0.478 | 59.62 | 0.7 | 0.1909 | 1.086 | 0.506 | 61.86 |
| 19 | 1.046 | 0.133 | 7.865 | 0.639 | 0.452 | 0.04 | 0.3859 | 17.13 | 0.432 | 4.63 | 0.01 | 0.3813 | 18.53 | 0.42 | 7.619 |
| 20 | 8.374 | 0.129 | 64.915 | 0.485 | 0.722 | 0.27 | 0.7201 | 0.259 | 1.683 | 57.1 | 0.2 | 0.7132 | 1.228 | 1.682 | 57.07 |
| 21 | 8.374 | 0.147 | 56.966 | 0.64 | 1.323 | 0.65 | 1.3015 | 1.654 | 3.497 | 62.17 | 0.6 | 1.3312 | 0.62 | 3.7344 | 64.57 |
| 22 | 8.374 | 0.147 | 56.966 | 0.41 | 0.598 | 0.2 | 0.5978 | 0.032 | 0.656 | 8.841 | 0.15 | 0.5974 | 0.107 | 1.219 | 50.94 |
| 23 | 2.932 | 0.023 | 127.48 | 0.456 | 0.169 | 0.19 | 0.1684 | 0.333 | 0.426 | 60.33 | 0.15 | 0.175 | 3.425 | 0.438 | 61.42 |
| 24 | 2.932 | 0.023 | 127.48 | 0.552 | 0.221 | 0.26 | 0.2207 | 0.139 | 0.65 | 66 | 0.2 | 0.2256 | 2.034 | 0.663 | 66.67 |
| 25 | 1.13 | 0.026 | 43.462 | 0.6 | 0.176 | 0.6 | 0.1766 | 0.365 | 0.431 | 59.16 | 0.4 | 0.1633 | 7.767 | 0.418 | 57.89 |
| Average deviation | | | | | | | | 3.079 | | 43.53 | | | 4.974 | | 49.31 |

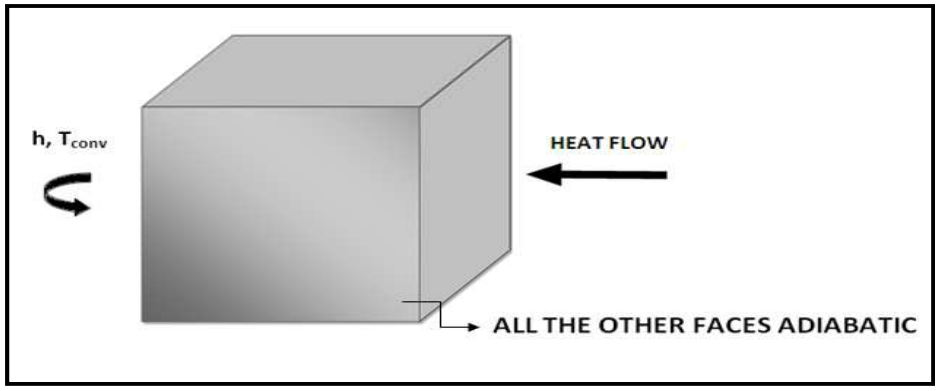


**Figure No.1: The Thermal boundary condition applied on the unit cell**

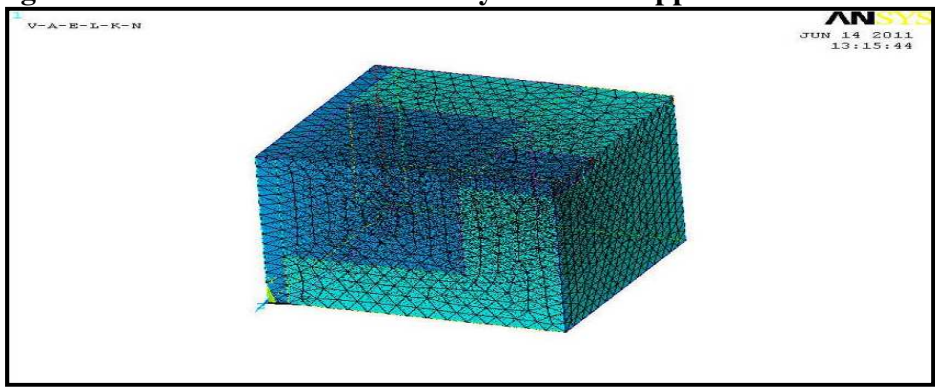


**Figure No.2: Meshed model of unit cell for square cylinder**

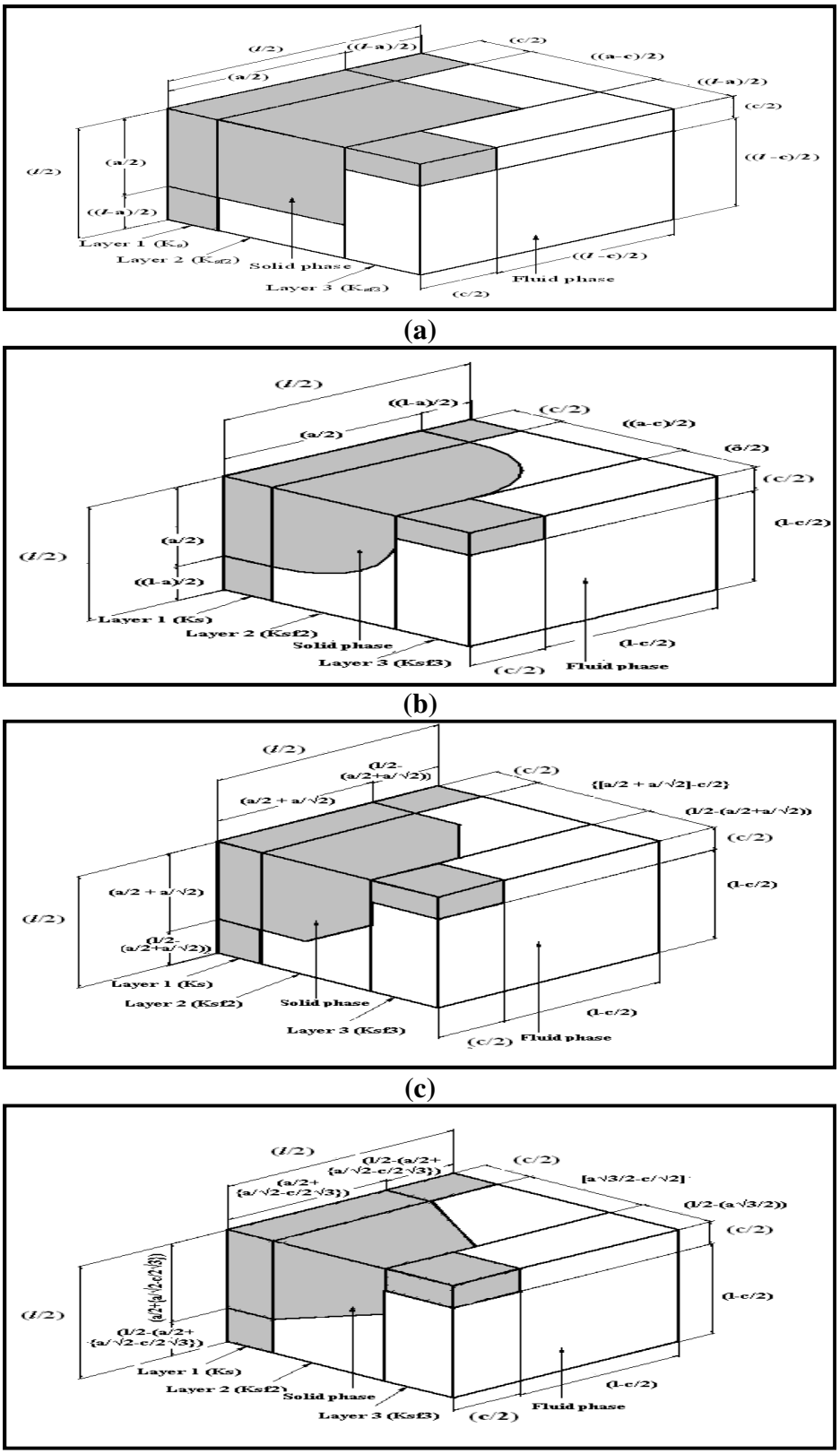


**Figure No.3: Two dimensional periodic two-phase system: (a) Square cylinder (b) Circular cylinder (c) Octagon cylinder (d) Hexagon cylinder**

## CONCLUSION

The comparison has been made between the constant and varying cross sections with available experimental data. It is clearly indicates that model with varying cross section predicts the effective thermal conductivity better than the model with constant cross section.

## ACKNOWLEDGEMENT

The authors wish to express their sincere gratitude to Department of Mechanical Engineering, PSG, College of Technology, Coimbatore, India for providing necessary facilities to carry out this research work.

## CONFLICT OF INTEREST

We declare that we have no conflict of interest.

## BIBLIOGRAPHY

1. Reddy K S, Karthikeyan P. Estimation of Effective Thermal Conductivity of Two-Phase Materials Using Collocated Parameter Model, *Heat Transfer Engineering,* 30(12), 2009, 998-1011.
2. Tai H. Equivalent thermal conductivity of two- and three-dimensional orthogonally fiber- reinforced composites in one-dimensional heat flow, *J Compos Technol Res,* 18(3), 1996, 221-227.
3. Jones W F, Pascal F. Numerical calculations of thermal conductivities of composites-a 3-D model, *Geophysics,* 60(4), 1995, 1038-1050.
4. Graham S, McDowell D L. Numerical analysis of the transverse thermal conductivity of composites with imperfect interfaces, *Transactions of the ASME, J Heat Transf,* 125(3), 2003, 389-393.
5. Krach A, Advani S G. Influence of void shape, void volume and matrix anisotropy on effective thermal conductivity of a three-phase composite, *J Compos Mater,* 30(8), 1996, 933-946.
6. Al-Sulaiman F A, Mokheimer E M A, Al-Nassar Y N. Prediction of the thermal conductivity of the constituents of fiber reinforced composite laminates, *J Heat mass Transfer,* 42(5), 2005, 370-377.
7. Zou M, Yu B, Zhang D. An analytical solution for transverse thermal conductivities of unidirectional fiber composites with thermal barrier, *J Phys D Appl Phys,* 35(15), 2002, 1867-1874.
8. Senthil Kumar A P, Prabhu Raja V, Karthikeyan P. "Effective Thermal Conductivity Modeling with Primary and Secondary parameters for Two phase materials", *Thermal Science,* 2(14), 2010, 393-407.
9. Senthil Kumar A P, Prabhu Raja V, Karthikeyan P. "Influence of primary and secondary parameters on thermal conductivity modeling for two phase materials", *International journal of Engineering,* 3, 2010, 255-262.

**Please cite this article in press as:** Senthil Kumar A P. Comparison of 2-d and 3-d effects on various geometry to predict the effective thermal conductivity of porous system, *International Journal of Engineering and Robot Technology,* 5(1), 2018, 6-12.